

Electronic Supplementary Material (ESI) for New Journal of Chemistry.

## Supporting Information

### Polyoxometalate@MIL-101/MoS<sub>2</sub>: a composite material based on MIL-101 platform with enhanced performances

Dadong Liang,<sup>a,b</sup> Chen Liang,<sup>a</sup> Lingkun Meng,<sup>a</sup> Yue Lou,<sup>a</sup> Chunguang Li<sup>a</sup> and Zhan Shi<sup>\*a</sup>

a. State Key Laboratory of Inorganic Synthesis and Preparative, College of Chemistry, Jilin University, Changchun, 130012, China. E-mail: zshi@mail.jlu.edu.cn

b. College of Resources and Environment, Jilin Agricultural University, Changchun, 130118, China. E-mail: [zshi@mail.jlu.edu.cn](mailto:zshi@mail.jlu.edu.cn)

#### S-1. Synthetic methods

##### S-1.1 Synthesis of MIL-101.

MIL-101 was synthesized according to the method reported previously.<sup>S1</sup> In brief, a mixture containing Cr(NO<sub>3</sub>)<sub>3</sub>·9H<sub>2</sub>O (0.40 g, 1.00 mmol), 1,4-benzenedicarboxylic acid (0.16 g, 0.96 mmol), hydrofluoric acid (1 mmol), and water (4.80 mL) was sealed in a Teflon autoclave and heated at 220 °C for 8 h. The product was washed by DMF and ethanol for several times and dried at 80 °C.

##### S-1.2 Synthesis of PW<sub>11</sub>Fe@MIL-101.

This preparation process of PW<sub>11</sub>Fe@MIL-101 is similar to that of PW<sub>11</sub>Fe@MIL-101/MoS<sub>2</sub>, except that MIL-101 was used for replacing MIL-101/MoS<sub>2</sub>.

#### S-2. Dye adsorption experiments

##### S-2.1 experiments

The adsorbents were dried under vacuum at 120 °C for 12h and then kept in a desiccator before the adsorption experiments. Taking the RhB adsorption experiments for example, the RhB aqueous solutions were prepared by dissolving solid RhB in ultrapure water. The adsorption experiments were performed under ambient conditions (298 ± 2 K) in the aqueous solutions. In a typical process, 100 mL of the RhB solution was stirred continually by a magnetic bar in the dark, and the adsorption test was started when 20 mg of the adsorbent was added. At per-determined time intervals, the supernatant was taken and analyzed using a UV-Vis spectrophotometer at the wavelength of 554 nm. During the adsorption kinetic experiments, the RhB solutions with the concentrations of 50, 100, and 200 mg L<sup>-1</sup>, respectively, were used. In the adsorption thermal isotherm studies, the concentrations of RhB varied from 50 to 400 mg L<sup>-1</sup>.

The amount of adsorbed dye at equilibrium,  $q_e$  (mg g<sup>-1</sup>), was calculated using the following equation:

$$q_e = \frac{(C_0 - C_e) \times V}{W} \quad (1)$$

where  $C_0$  (mg L<sup>-1</sup>) and  $C_e$  (mg L<sup>-1</sup>) mean the initial and equilibrium concentrations of RhB, respectively.  $V$  (L) and  $W$  (g) mean the volume of the RhB solution and the weight of the

adsorbent, respectively.

### S-2.2 Adsorption kinetics.

The adsorption kinetics of RhB on the adsorbents were studied using two common models: pseudo-first-order, pseudo-second-order:

Pseudo-first-order equation:

$$\lg(q_e - qt) = \lg q_e - \frac{K_1}{2.303} t \quad (2)$$

where  $q_e$  ( $\text{mg g}^{-1}$ ) and  $qt$  ( $\text{mg g}^{-1}$ ) are the adsorption capacities at equilibrium and time  $t$  (min), respectively.  $K_1$  ( $\text{g mg}^{-1} \text{min}^{-1}$ ) is the kinetic rate constant.

Pseudo-second-order kinetic equation:

$$\frac{t}{q_e} = \frac{1}{K_2 q_e^2} + \frac{t}{q_e} \quad (3)$$

where  $K_2$  ( $\text{g mg}^{-1} \text{min}^{-1}$ ) is the second-order rate constant.

### S-2.3 Adsorption thermodynamic.

Two most frequently used isotherm models were selected to fit the data of adsorption experiments, which are Langmuir and Freundlich isotherm models. They were expressed in the following equation.

The Langmuir isotherm equation:

$$\frac{1}{q_e} = \frac{1}{C_e K_L q_m} + \frac{1}{q_m} \quad (5)$$

Where  $K_L$  ( $\text{L mg}^{-1}$ ) is Langmuir constant,  $q_m$  ( $\text{mg g}^{-1}$ ) is the maximum adsorption capacity.

Freundlich equation:

$$\lg q_e = \lg K_F + \frac{1}{n} \lg C_e \quad (6)$$

where  $K_F$  and  $n$  are Freundlich constants.<sup>S2</sup>

### S-2.4 Regeneration and reuse of PW<sub>11</sub>Fe@MIL-101/MoS<sub>2</sub>.

The used adsorbent was recovered from the RhB aqueous solution by centrifugation. Before the adsorbent was reused, it was repeatedly washed with the aqueous solution of NaCl and DMF. This method was reported in previous paper.<sup>S3</sup> After the adsorbent was immersed in the NaCl aqueous solution, RhB cations could be partially removed through the cation-exchange process. Moreover, RhB could be further removed after the sample was washed with DMF because of the high solubility of RhB in DMF. The detailed desorption processes can be described as follows. The used PW<sub>11</sub>Fe@MIL-101/MoS<sub>2</sub> sample was dispersed in the aqueous solution of NaCl (0.5 M) and stirred for tens of mins. Then, it was separated, dispersed in DMF, and further stirred for another tens of mins. As shown Fig. S12, RhB could be effectively removed from the adsorbent through being treated in the NaCl aqueous solution and DMF, respectively. These processes were carried out repeatedly until no adsorption peaks of RhB were observed in the UV-vis spectra, which indicates that the removable RhB molecules have been fully desorbed from the adsorbent. Finally, the adsorbent was washed with ethanol to remove DMF from the sample. The regenerated sample was dried overnight at 393 K under vacuum before it was reused for the next adsorption experiments.

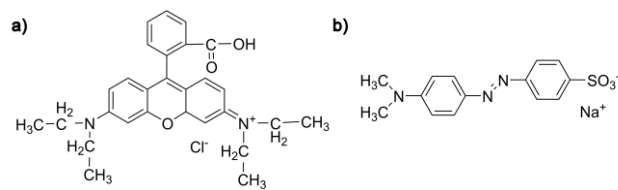


Fig. S1. The structures of a) RhB and b) MO.

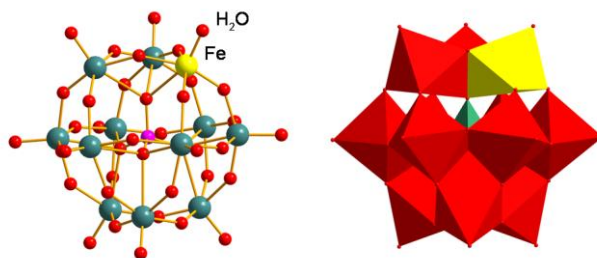


Fig. S2. The structural images of  $PW_{11}Fe$ .

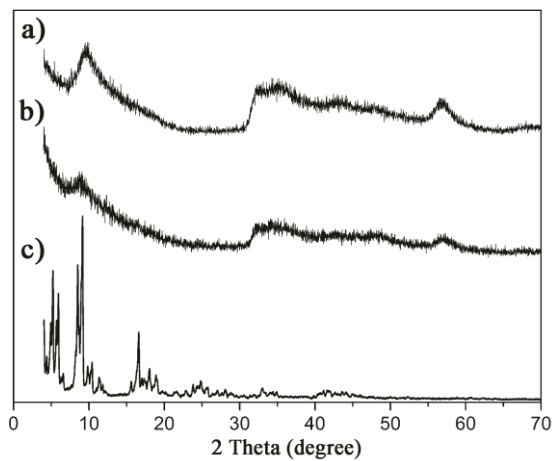


Fig. S3. The XRD patterns of (a)  $MoS_2$  synthesized using  $Na_2MoO_4$  and  $C_2H_5NS$  as the reactants, (b) the sample obtained through treating MIL-101 in the solution containing  $Na_2MoO_4$  and  $C_2H_5NS$  under microwave irradiation, and (c) MIL-101.



Fig. S4. Image of the samples of MIL-101/MoS<sub>2</sub> (left) and MIL-101 (right).

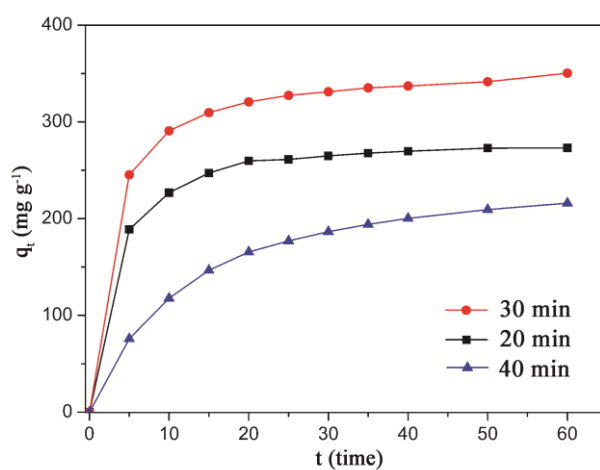


Fig. S5. The adsorption capacities of RhB over MIL-101/MoS<sub>2</sub> samples synthesized with different reaction time.

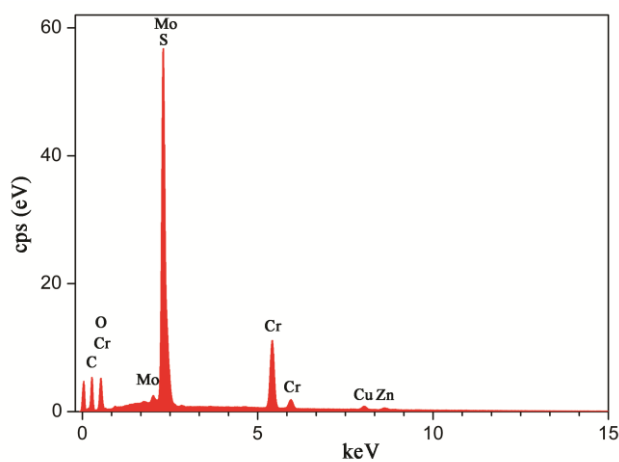


Fig. S6. EDS spectrum of MIL-101/MoS<sub>2</sub>. During the process of EDS analysis, the sample was dispersed on the Cu-Zn alloy.

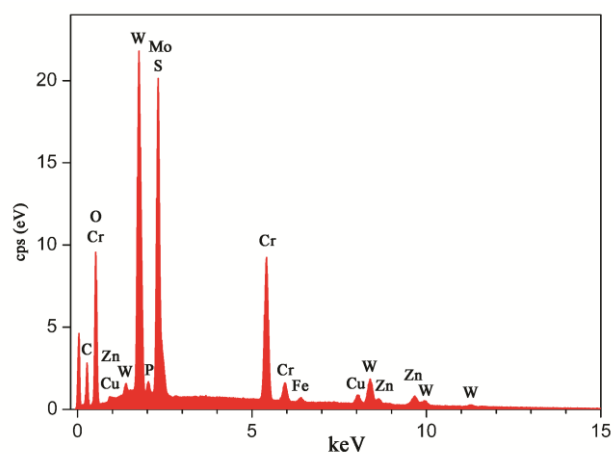


Fig. S7. EDS spectrum of  $PW_{11}Fe@MIL-101/MoS_2$ .

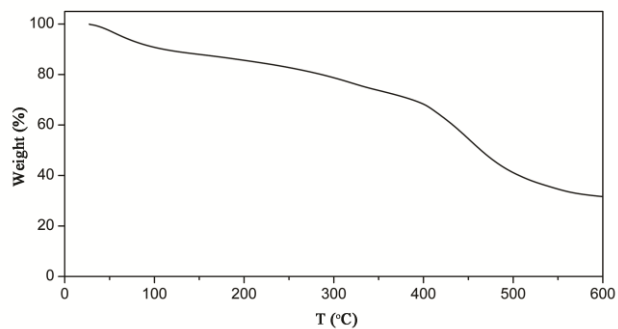


Fig. S8. The TG curve of  $PW_{11}Fe@MIL-101/MoS_2$ .

Table S1. Kinetic model parameters of RhB adsorption onto MIL-101/ $MoS_2$ .

$c_o$ ( $mg\ L^{-1}$ )	$q_{e,exp}$ ( $mg\ g^{-1}$ )	Pseudo-first-order kinetic		Pseudo-second-order kinetic	
		$q_{e,cal}$ ( $mg\ g^{-1}$ )	$R^2$	$q_{e,cal}$ ( $mg\ g^{-1}$ )	$R^2$
50	140.81	44.22	0.9841	144.93	0.9999
100	236.39	53.22	0.8858	238.10	0.9998
200	355.83	105.56	0.9521	357.14	0.9997

Table S2. Comparison for the removal of RhB by various adsorbents.

Adsorbents	Adsorption capacity (mg g <sup>-1</sup> )	Reusability	Ref.
MIL-68(Al)	1111.11 <sup>a</sup>	Yes	S4
[H <sub>2</sub> N(Me) <sub>2</sub> ][Ln <sub>3</sub> (OH)(bpt) <sub>3</sub> (H <sub>2</sub> O) <sub>3</sub> ](DMF) <sub>2</sub> ·(H <sub>2</sub> O) <sub>4</sub>	735 <sup>b</sup>	No report	S5
PW <sub>11</sub> Fe@MIL-101/MoS <sub>2</sub>	560 <sup>c</sup>	Yes	This work
MIL-101/MoS <sub>2</sub>	500 <sup>a</sup>	Yes	This work
MoS <sub>2</sub> /MIL-101	344.8 <sup>a</sup>	Yes	S6
MIL-68(In)-NH <sub>2</sub> /graphite oxide composite	267 <sup>a</sup>	Yes	S7
Ni doped FeO(OH)-NWS-AC	210.17 <sup>a</sup>	No report	S8
Zn(phenDIB)(AOBTC) <sub>0.5</sub>	127.5 <sup>a</sup>	Yes	S9
Graphene oxide	154.8 <sup>a</sup>	No report	S10
Graphene oxide/Beta zeolite composite	64.47 <sup>a</sup>	Yes	S11
MIL-125(Ti)	59.92 <sup>a</sup>	No report	S12
Sodium montmorillonite	42.19 <sup>a</sup>	No report	S13
Reduced Graphene oxide/ZnO	32.6 <sup>a</sup>	Yes	S14
Beta Zeolite	27.94 <sup>a</sup>	Yes	S11
Zeolite	13.22 <sup>a</sup>	Yes	S15
MCM-22	0.054 <sup>a</sup>	No report	S16

a. maximum adsorption capacity; b. RhB concentration, 300 mg L<sup>-1</sup>; c. RhB concentration, 400 mg L<sup>-1</sup>.

Table S3. Kinetic model parameters of RhB adsorption onto PW<sub>11</sub>Fe@MIL-101/MoS<sub>2</sub>.

c <sub>0</sub> (mg L <sup>-1</sup> )	q <sub>e,exp</sub> (mg g <sup>-1</sup> )	Pseudo-first-order kinetic		Pseudo-second-order kinetic	
		q <sub>e,cal</sub> (mg g <sup>-1</sup> )	R <sup>2</sup>	q <sub>e,cal</sub> (mg g <sup>-1</sup> )	R <sup>2</sup>
50	186.23	38.68	0.9361	188.68	0.9999
100	373.34	105.80	0.9811	384.62	0.9999
200	520.25	121.73	0.9397	526.32	0.9998

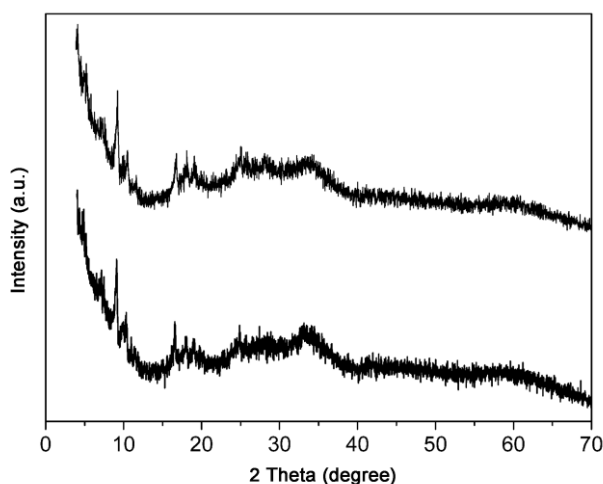


Fig. S9. XRD of as-synthesized sample (upper) and regenerated sample (lower) of PW<sub>11</sub>Fe@MIL-101/MoS<sub>2</sub>.

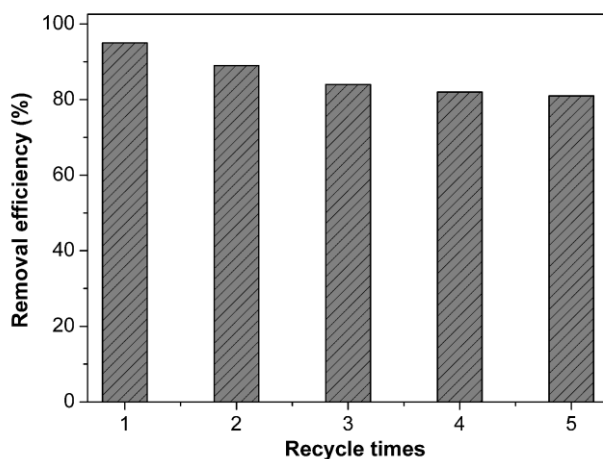


Fig. S10. The reusability of  $PW_{11}Fe@MIL-101/MoS_2$  for removal of RhB.

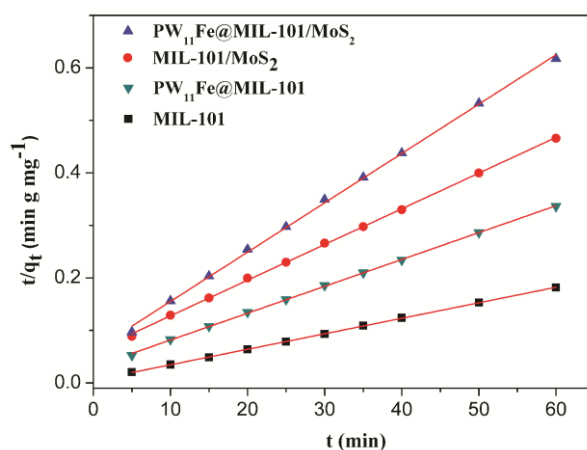


Fig. S11. Plots of pseudo-second-order kinetics of MO adsorption over MIL-101,  $PW_{11}Fe@MIL-101$ ,  $MIL-101/MoS_2$ , and  $PW_{11}Fe@MIL-101/MoS_2$  (MO,  $200 \text{ mg L}^{-1}$ ; adsorbents,  $0.2 \text{ g L}^{-1}$ ).

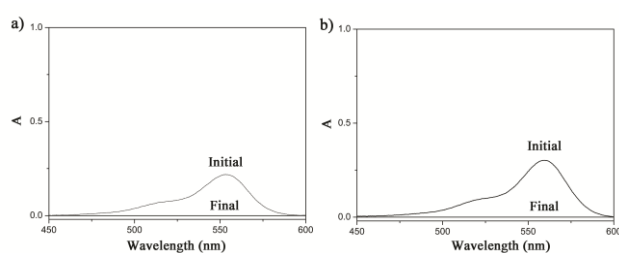


Fig. S12. The UV-vis spectra of filtrates ((a) NaCl aqueous solution and (b) DMF) used in the desorption processes of RhB from  $PW_{11}Fe@MIL-101/MoS_2$ .

## References

- S1 G. Férey, C. Mellot-Draznieks, C. Serre, F. Millange, J. Dutour, S. Surblé, I. Margiolaki, *Science*, 2005, **309**, 2040-2042.
- S2 S. Chowdhury, R. Mishra, P. Saha, P. Kushwaha, *Desalination*, 2011, **265**, 159-168.
- S3 A. X. Yan, S. Yao, Y. G. Li, Z. M. Zhang, Y. Liu, W. L. Chen and E. B. Wang, *Chem. Eur. J.*, 2014, **20**, 6927-6933.

- S4 M. S. Tehrani, R. Zare-Dorabei, *RSC Adv.*, 2016, **6**, 27416-27425.
- S5 S. H. Xing, Q. M. Bing, L. F. Song, G. H. Li, J. Y. Liu, Z. Shi, S. H. Feng, R. R. Xu, *Chem. Eur. J.*, 2016, **22**, 16230–16235.
- S6 G. Yang, J. H. Cheng, Y. C. Chen and Y. Y. Hu, *J. Colloid. Interf. Sci.*, 2017, **504**, 39-47.
- S7 C. Yang, S. Wu, J. Cheng, Y. Chen, *J. Alloy. Compd.*, 2016, **687**, 804-812.
- S8 F. N. Azad, M. Ghaedi, A. Asfaram, A. Jamshidi, G. Hassani, A. Goudarzi, M. H. A. Azqhandi and A. Ghaedi, *RSC Adv.*, 2016, **6**, 19768–19779.
- S9 M. K. Wu, F. Y. Yi, Y. Feng, X. W. Xiao, S. C. Wang, L. Q. Pan, S. R. Zhu, K. Tao, L. Han, *Cryst. Growth Des.*, 2017, **17**, 5458-5464.
- S10 Q. Q. Jin, X. H. Zhu, X. Y. Xing, T. Z. Ren, *Adsorpt. Sci. Technol.*, 2012, **30**, 437-448.
- S11 Z.L. Cheng, Y.X. Li, Z. Liu, *J. Alloy. Compd.*, 2017, **708**, 255-263.
- S12 H. Guo, F. Lin, J. Chen, F. Li and W. Weng, *Appl. Organomet. Chem.*, 2015, **29**, 12–19.
- S13 P. P. Selvam, S. Preethi, P. Basakaralingam, N. Thinakaran, A. Sivasamy and S. Sivanesan, *J. Hazard. Mater.*, 2008, **155**, 39–44.
- S14 J. Wang, T. Tsuzuki, B. Tang, X. Hou, L. Sun, X. Wang, *ACS Appl. Mat. Inter.*, 2012, **4**, 3084-3090.
- S15 S. Wang, Z. H. Zhu, *J. Hazard. Mater.*, 2006, **136**, 946-952.
- S16 S. Wang, H. Li and L. Xu, *J. Colloid Interface Sci.*, 2006, **295**, 71–78.